Radiation damage in nanocrystalline Ni under irradiation studied using positron annihilation spectroscopy

AUTHOR(S):

Tsuchida, H.; Iwai, T.; Awano, M.; Oshima, N.; Suzuki, R.; Yasuda, K.; Batchuluun, C.; Itoh, A.

Radiation damage in nanocrystalline Ni under irradiation studied using positron annihilation spectroscopy

H. Tsuchida[1,*], T. Iwai[2], M. Awano[3], N. Oshima[4], R. Suzuki[4]
K. Yasuda[5], C. Batchuluun[5], and A. Itoh[1]

[1]Quantum Science and Engineering Center, Kyoto University, Uji, Kyoto 611-0011, Japan
[2]Nuclear Professional School, School of Engineering, The University of Tokyo, Ibaraki 319-1188, Japan
[3]Department of Physics, Nara Women's University, Nara 630-8506, Japan
[4]Research Institute of Instrumentation Frontier (RIIF), National Institute of Advanced Industrial Science and Technology (AIST), Tsukuba, Ibaraki 305-8568, Japan
[5]The Wakasa wan Energy Research Center, Tsuruga, Fukui 914-0192, Japan

*Corresponding author

Keywords: in situ observation; positron annihilation spectroscopy; nanocrystalline materials

PACS codes: 61.72.Ji, 61.80.-x, 61.82.Rx, 78.70.Bj

Abstract

We studied the grain size dependence of the defect evolution that occurred in a nanocrystalline (NC) Ni and its coarse-grained counterpart under irradiation. The vacancy defects produced during irradiation were investigated via in situ observations of the positron annihilation Doppler broadening spectra. The annihilation line-shape

parameter *S* was measured under beam-on (during irradiation) and beam-off (after irradiation) conditions. We found that different variations in *S* were observed depending on the grain size; for the coarse-grained specimen, the *S* measured under beam-on conditions was larger than that observed under beam-off conditions, while for the NC specimen, the *S* value remained unchanged under beam-on and beam-off conditions. The former result indicated that the vacancy concentration was enhanced during irradiation, due to transient vacancy production. The latter result may imply that defect accumulation was strongly suppressed under irradiation. We also studied the flux dependence of the radiation damage effects for the NC specimen, using high-flux He ions in the flux range of 1.2×10^{13} to 6×10^{14} ions/($cm^2 \cdot s$). A slight flux dependence was observed, which was due to microstructural changes at the intersections of the crystallite interfaces under the highest flux irradiation studied.

1. Introduction

Materials in fusion reactors or nuclear reactors are used in an irradiating environment. In such an environment, a variety of radiation damage effects occur in the collision cascade region, including defect production, vacancy-interstitial recombination, and the absorption of defects by sinks. Consequently, the defect concentrations and microstructures are varying continuously during irradiation. A fundamental understanding of the dynamic evolution of defects during irradiation is therefore important for the development of radiation-resistant materials.

Nanocrystalline (NC) materials are known to have high resistance to radiation damage effects, because the grain boundaries act as effective sinks that absorb radiation-induced defects. A number of studies have made experimental and theoretical investigations of the radiation resistance of various NC materials [1,2]. Most of the experimental investigations have focused on the changes in microstructure after irradiation. Recent simulations using a molecular dynamics method showed that a new mechanism of radiation resistance in NC materials—namely, the self-healing of radiation damage—occurs near grain boundaries during irradiation, via interstitial emission [3].

Recently, we reported experimental results for the real-time observation of defect production in polycrystalline Ni specimens during irradiation, using positron annihilation spectroscopy [4,5]. The results showed that the concentration of vacancies during irradiation was high, compared with the concentration of vacancies surviving after irradiation. This indicated that transient vacancy defects were produced during irradiation, leading to an increase in the concentration of vacancies during irradiation. Although the vacancies that survived after irradiation vanished at high temperatures (713 K) when vacancy-interstitial recombination occurred (annealing effects), the transient vacancies survived even at these temperatures. In addition, the transient vacancy production played a vital role in the void nucleation processes resulting from the nanometer-sized void production.

In this work, we investigated the production of transient vacancies for an NC in an ion-irradiation environment. Two kinds of irradiation experiments were performed: (1) the in situ observation of defects produced during irradiation with MeV-energy C ions; and (2) measurements of the structural modification at grain boundaries under high-flux

He-ion irradiation. We focused on the radiation damage effects at grain boundaries in the NC materials. The structures of the free volumes in the NC materials were studied using positron annihilation spectroscopy (both the annihilation γ-ray Doppler broadenings and the positron lifetimes were measured). The present results provided information not only on the sink strength of transient vacancies into grain boundaries, but also the stability of transient vacancies in nano-structured materials.

2. Experimental

An NC Ni foil with a thickness of 10 μm supported by a copper sheet, obtained from the Goodfellow Company, UK, was used as a target specimen. The specimen purity was 99.0%. The specimen was made using the electro deposition method [6]. The average grain size in the NC specimen was 30 nm, measured using a transmission electron microscope (TEM) operated at 200 kV. A coarse-grained Ni specimen with an average grain size of a few micrometers was prepared by annealing a rolled Ni foil (purity of 99.4%) at 1173 K for 1 hour in vacuum.

Two kinds of irradiation experiments were performed, as follows. First, in situ measurements of the positron annihilation Doppler broadenings were made during irradiation. The experiments were carried out with 0.5 and 2.5 MeV C ions at the High Fluence Irradiation Facility, the University of Tokyo. The experimental procedures used were essentially the same as those described in our previous studies [4-5]. The experimental system consisted of a slow-positron-beam apparatus and a MeV-energy ion accelerator, enabling in-situ probing of the radiation-induced defects under

irradiation. The specimens used were NC Ni, and its coarse-grained polycrystalline counterpart. The Doppler broadening spectra were measured alternately during and before/after irradiation. The spectrum was characterized by the line-shape parameter *S*, which is defined as the ratio of the counts in the central position of the annihilation photopeak (ranging from 510.2 to 511.8 keV) to the total counts in the peak (from 507.0 to 515.0 keV). In the spectrum, the total counts measured from the photo-peak area were 10^5 or more. The overall experimental errors for *S* due to statistical errors were ±0.003. In each run of annihilation spectrum measurements, data were collected for 10 or 15 minutes; this time was changed according to the count rate of the annihilation γ-rays. The average fluence received by sample after single irradiation run was on the order of 10^{14} ions/cm^2.

The other experiments involved the irradiation of the NC specimen with high-flux 190 keV He beams. The experiment was performed at the Wakasa-wan Energy Research Center, Japan. The specimens were irradiated at three different fluxes of 1.3×10^{13}, 6.3×10^{13}, and 6.3×10^{14} He ions/(cm^2·s), under a constant fluence of 1.8×10^{16} He ions/cm^2. The target temperature during irradiation was monitored using a thermocouple. The maximum target temperatures were 318, 328, and 345 K for the fluxes of 1.3×10^{13}, 6.3×10^{13}, and 6.3×10^{14} He ions/(cm^2·s), respectively. It should be noted that no changes in grain size or microstructure (grain growth) occurred at these temperatures [7]. To identify the defects formed after irradiation, positron lifetime spectroscopy measurements were performed at the intense slow positron beam facility of the National Institute of Advanced Industrial Science and Technology, Japan. In the lifetime measurement system, the time resolution was ~250 ps [8]. We also studied the depth

profile of defects by measuring the *S* parameter as a function of the positron incident energy.

Figure 1 shows the irradiation conditions for the two experiments mentioned above, in terms of the radiation damage distributions (the number of vacancies produced by one projectile ion) and positron implantation profiles, where the damage distribution by ions was calculated using the transport of ions in matter (TRIM) code [9], and the positron implantation profile was calculated using the formula described by Puska *et al*. [10]. To study the defect density-dependence of the microstructural stability in the NC material, we chose a specific combination of incident energies of projectile ions and positrons. In the case shown in Fig. 1 (a), the positron probing region overlapped with the tail of the damage distributions (which corresponded to the damage region of low defect density). In contrast, in Fig. 1 (b) and (c), one can see that both the profiles completely overlapped, showing that positron probing occurred in all of the radiation damage regions.

3. Results and discussion

We investigated the behavior of the defects produced during irradiation. Figure 2 shows experimental results for the sequential variation of the annihilation line parameter *S* under beam-on (during irradiation) and beam-off (before/after irradiation) conditions for the NC specimen irradiated with 0.5 and 2.5 MeV C ion beams, and for the coarse-grained specimen irradiated with 2.5 MeV C ions. The closed and open symbols denote the *S* parameter measured under beam-on and beam-off conditions, respectively.

In each irradiation period, the average fluxes were 1.9×10^{11} and 5.2×10^{11} ions/(cm^2·s) for 2.5 and 0.5 MeV C ions, respectively. In both cases, the temperature rise of the target specimen during irradiation was less than 10 K, indicating that the beam-heating effect was of minor importance. In the un-irradiated specimens (Run 1 shown in Fig. 2(a) and (b)), *S* had a high value of approximately 0.49, because positrons were trapped at the existing defects. In contrast, for the coarse-grained specimen prepared using annealing (Run 1 shown in Fig. 2(c)) the measured *S* corresponded to that observed for the positron annihilation in the bulk.

The variation of *S* for the NC specimen was different from that observed for the coarse-grained specimen. For the coarse-grained specimens, the *S* measured during irradiation was larger than that observed before/after irradiation, while for the NC specimens, the *S* value remained unchanged. The results for the coarse-grained specimens indicated that the concentration of vacancies during irradiation was high compared with that after irradiation. This was due to the fact that transient vacancy defects were produced during irradiation, as observed in our previous studies [4,5]. In contrast, the results for the NC specimens suggested that such transient vacancies disappeared, and the defect concentration remain unchanged during irradiation. It is reasonable to believe that the transient vacancies formed during irradiation were unstable in the NC materials, and were annihilated by strong sinks at the grain boundaries, or via recombination with interstitials.

To characterize the microstructural changes (defect types at interfaces) induced by irradiation, we performed positron lifetime measurements for the NC specimen after the irradiation experiments (Run 13 shown in Fig. 2 (a) and (b)). The specimens were

irradiated at total fluences (the corresponding displacements per atom) of 2.8×10^{15} ions/cm^2 (3.3×10^{-1} dpa) and 1.0×10^{15} ions/cm^2 (3.2×10^{-2} dpa), for 0.5 and 2.5 MeV C ion irradiation, respectively. The incident positron energies were the same as those used in the in situ positron-annihilation experiments. The lifetime spectra were analyzed using two components, τ_1 and τ_2, where the first lifetime τ_1 is attributed to positron trapping at the free volumes in the crystalline interfaces, and the second lifetime τ_2 is due to the free volumes at the intersections of two or three crystallite interfaces [6]. The lifetimes obtained are listed in Table 1. The result for the un-irradiated specimen was in good agreement with that obtained by Petegem *et al*. [6], where the τ_1 of approximately 162 ps and the τ_2 of 340-350 ps corresponded to free volumes with the approximate size of a single vacancy, and those with the size of a cluster of 10-15 vacancies, respectively. Comparing the irradiated and un-irradiated samples, the τ_1 values were almost the same, within the experimental uncertainty. The τ_2 values (again, corresponding to a free volume with a size equivalent to 15-20 vacancies) increased significantly as the total ion fluence (or the dpa) increased. This may have been due to the growth of microvoids.

Next, we discuss the radiation damage in NC materials under high-flux He irradiation. In this irradiation experiment, we used three different fluxes (or dpa rates) of 1.3×10^{13} (2.2×10^{-3}), 6.3×10^{13} (1.1×10^{-2}), and 6.3×10^{14} ions/(cm^2·s) (1.1×10^{-1}). The total ion fluence was kept constant at 1.8×10^{16} ions/cm^2. We estimated intervals of ion irradiation for a single grain corresponding to the fluxes studied, *T*. Assuming that the grains were spherical, the cross section of one grain was 7.1×10^{-12} cm^2, where the average radius of the grains was 15 nm, from the TEM observation. The obtained values of *T* were 11, 2.2, and 0.22 ms for fluxes of 1.3×10^{13}, 6.3×10^{13}, and 6.3×10^{14} He

ions/(cm^2·s), respectively. It should be noted that for the highest flux irradiation the time interval of 0.22 ms was comparable with the time scale of the diffusion phase in the relaxation sequence of radiation-induced defects [11]. In such a situation, the defect evolution may have been enhanced, because the defect production under irradiation occurred simultaneously with the defect relaxation.

Table 2 shows the results from the positron lifetime analysis for specimens after irradiation. It can be seen that the τ_1 values for the irradiated specimens increased compared with those for the un-irradiated specimens. Interestingly, the τ_2 values observed for He ion irradiation with a high dpa of approximately 3.2 were clearly shorter than those for C ion irradiation with a low dpa of approximately 0.33 or 0.032 (see Table 1). The τ_2 value for C ion irradiation was approximately 370 ps, while for He ion irradiation it was approximately 310 ps. This may have been due to the absorption of He atoms into free volumes at the intersections of two or three crystallite interfaces (triple junctions), leading to a decrease in positron lifetime. For instance, according to the calculation described by Shivachev *et al*. [12], the positron lifetime value of 350 ps for a void containing 12 vacancies was reduced to approximately 300 ps for three He atoms contained in the void.

In addition, one can see that the mean positron lifetime increased slightly with increasing flux. It is well known that the mean positron lifetime is correlated with the positron diffusion length [13]. To study this increase in more detail, we performed measurements of the *S* parameter at different incident positron energies *E* (*S*-*E* curve) for the NC materials after irradiation. We estimated the positron diffusion length *L* from

the *S*-*E* curve results, following the back-diffusion trapping model [14]. The measured *S* parameter is expressed as a function of the incident positron energy, *E*, as follows:

$$S(E) = S_s F(E) + S_b(1 - F(E)), \quad (1)$$

where S_s is the value of the line-shape parameter for annihilation at a surface region, and S_b the value for annihilation in a bulk region. $F(E)$ is the fraction of positrons diffusing back to the surface as a function of the incident position energy *E*. The back-diffusing fraction of positrons is a function of not only the positron implantation depth, but also the defect concentration. $F(E)$ is given by

$$F(E) = \int_0^\infty P(z,E)\exp(-z/E)dz. \quad (2)$$

$P(z, E)$ is the implantation profile of monoenergetic positrons with energy *E*, $P(z,E) = m\,z^{m-1}/z_0^m\,exp[-(z/z_0)^m]$ with $z_0 = A\,E^n/(\rho\Gamma(1-1/m))$, where ρ is the mass density of material, Γ the gamma function, and z_0 is the mean implantation depth. We used values of ρ = 8.90 g cm^{-3} for Ni and the Makhov profile parameters of A = 4.0 g cm^{-2} keV$^{-1.6}$, m = 2, and n = 1.6 [15]. In the fitting calculation, the value of S_s was taken as the *S* measured at 1 keV, and S_b was taken as the average of the *S* values measured in the energy range from 15 to 19 keV. We obtained a value for *L* by fitting the experimental data to equations (1) and (2). The results are shown in Fig. 3. The solid lines show the best fits to the data. For the un-irradiated specimen, the calculated value of *L* was almost the same as the mean grain size of the NC specimen used (approximately 30 nm). The *L* for the specimens irradiated at fluxes of 1.3 × 10^{13} and 6.3 × 10^{13} ions/(cm^2·s) remained unchanged compared with that for the un-irradiated specimen. Interestingly, for the highest flux of 6.3 × 10^{14} ions/(cm^2·s), *L* was 70 ± 10

nm, approximately twice as long as the L for the un-irradiated specimen. This meant that a microstructural change occurred at the interfaces of the grain boundaries.

4. Conclusion

We investigated the dependence of the grain size on the formation of transient vacancy defects that occurred during irradiation in a real-time Doppler-broadening positron-annihilation spectroscopy study. The radiation resistance in NC materials under high-flux helium irradiation was also studied. It was found that: (1) the transient vacancies were unstable in NC materials, and they could be annihilated at grain boundaries or via recombination with freely migrating interstitials during irradiation. (2) The implanted He atoms tended to accumulate at intersections or triple junctions in the NC materials. And (3) an analysis of the positron diffusion length showed that the microstructure at the grain boundaries changed slightly under irradiation with a high dpa rate, even for irradiation at the same fluence.

Acknowledgments

We thank T. Omata of The University of Tokyo for his technical support during the irradiation experiments. We also gratefully acknowledge Professor Ichiro Katayama of Institute of Particle and Nuclear Studies (KEK) for valuable discussions, and Professor Toshimasa Yoshiie of Research Reactor Institute, Kyoto University and Professor Masao Komatsu of Hiroshima Institute of Technology for their technical support for the TEM observations, and useful comments. This work was supported partly by a Japan

Society for the Promotion of Science (JSPS) Grant-in-Aid (Grant No. 17560742), and by contributions from Kansai Atomic Energy Council.

References

[1] M. Rose, G. Gorzawski, G. Miehe, A. G. Balogh, H. Hahn, NanoStruct. Mater. **6** (1995) 731-734

[2] M. Samaras, P. M. Derlet, H. Van Swygenhoven, M. Victoria, J. Nucl. Mater. **351** (2006) 47-55

[3] X. M. Bai, A. F. Voter, R. G. Hoagland, M. Nastasi and B. P. Uberuaga, Science 327 (2010) 1631-1634

[4] H. Tsuchida, T. Iwai, M. Awano, M. Kishida, I. Katayama, S.C. Jeong, H. Ogawa, N. Sakamoto, M. Komatsu, A. Itoh, J. Phys. Condens. Matter 19 (2007) 136205

[5] H. Tsuchida, T. Iwai, S. Kasai, H. Tanaka, N. Oshima, R. Suzuki, T. Yoshiie, A. Itoh, J. Phys. Conf. Series 262 (2011) 012060

[6] S. Van Petegem, F. Dalla Torre, D. Segers, H. Van Swygenhoven, Scripta Materialia **48** (2003) 17-22

[7] N. Nita, R. Schaeublin, M. Victoria, J. Nucl. Mater. **329-333** (2004) 953-957

[8] R. Suzuki, K. Kobayashi, T. Mikado, H. Ohgaki, M. Chiwaki, T. Yamazaki, T. Tomimasu, Jpn. J. Appl. Phys. 30 (1991) L532-534

[9] J. Zieglar, J. F. Biersack, U. Littmark, *The Transport of Ions in Matter (TRIM) Monte-Carlo calculation* including in Computer program SRIM Version 2008

(www.SRIM.org)

[10] M. J. Puska and R. M. Nieminen, Rev. Mod. Phys. **66** (1994) 841-897

[11] S. Ishino, J. Nucl. Mater. **206** (1993) 139-155

[12] B. L. Shivachev, T. Troev, T. Yoshiie, J. Nucl. Mater. **306** (2002) 105-111

[13] J. Dryzek, Phys. Stat. Sol. (b) **229** (2002) 1163-1173

[14] D. T. Britton, P. C. Rice-Evans, J. H. Evans, Phil. Mag. Lett. **57** (1988) 165-169

[15] A. Vehanen, K. Saarinen, P. Hautojärvi, H. Huomo, Phys. Rev. B **35** (1987) 4606-4610

Figure Captions

Fig. 1. Depth profiles of vacancy defects produced by one projectile ion, and positron implantation for combinations of (a) 2.5 MeV C ions and 15 keV positrons; (b) 0.5 MeV C ions and 20 keV positrons; and (c) 190 keV He ions and 20 keV positrons.

Fig. 2. Variation of the line-shape parameter *S* measured alternately under ion irradiation (closed symbols) and non-irradiation (open symbols) conditions, for (a) the NC Ni irradiated with 0.5 MeV C ions, (b) the NC Ni irradiated with 2.5 MeV C ions, and (c) the coarse-grained Ni irradiated with 2.5 MeV C ions. That data from Run 1 shows the results for un-irradiated specimens.

Fig. 3. The line-shape parameter *S* as a function of the incident positron energy, for the NC Ni materials irradiated with 190 keV He ions at a fixed fluence of 1.8×10^{16} He ions/cm^2; (a) un-irradiated, and irradiated at fluxes of (b) 1.3×10^{13} ions/(cm^2·s), (c) 6.3×10^{13} ions/(cm^2·s), and (d) 6.3×10^{14} ions/(cm^2·s). The solid lines show fitting curves obtained from a back-diffusion trapping model. The values for *L* are the positron diffusion lengths obtained from the best fits to the data.

Tables

Table 1: Positron lifetimes observed after irradiation, for nanocrystalline Ni irradiated with 0.5 and 2.5 MeV C ions. The value of the total dpa was 0.33 and 0.032 for 0.5 and 2.5 MeV C ions, respectively.

Samples	**τ_1 (ps)**	**τ_2 (ps)**	**I_1 (%)**	**I_2 (%)**
Unirradiated	162 ± 3 [a)]	341 ± 8 [a)]	71 ± 2 [a)]	29 ± 2 [a)]
	162 ± 3 [b)]	348 ± 11 [b)]	71 ± 4 [b)]	30 ± 4 [b)]
Irradiated with 2.5 MeV C ions	163 ± 3 [a)]	367 ± 8 [a)]	67 ± 3 [a)]	33 ± 3 [a)]
Irradiated with 0.5 MeV C ions	167 ± 4 [b)]	380 ± 10 [b)]	74 ± 4 [b)]	26 ± 4 [b)]

a) positron energy: 15 keV, b) positron energy: 20 keV

Table 2: Positron lifetimes for nanocrystalline Ni irradiated with 190 keV He ions at three different dpa rates. The value of the total dpa is 3.2.

DPA rate	**τ_1 (ps)**	**τ_2 (ps)**	**τ_{av} (ps)**	**I_2 (%)**
Unirradiated	161 ± 5	323 ± 4	210 ± 8	30 ± 2
2.2×10^{-3}	176 ± 6	312 ± 7	228 ± 15	38 ± 4
1.1×10^{-2}	179 ± 3	312 ± 5	228 ± 11	37 ± 3
1.1×10^{-1}	179 ± 3	315 ± 8	229 ± 18	37 ± 5

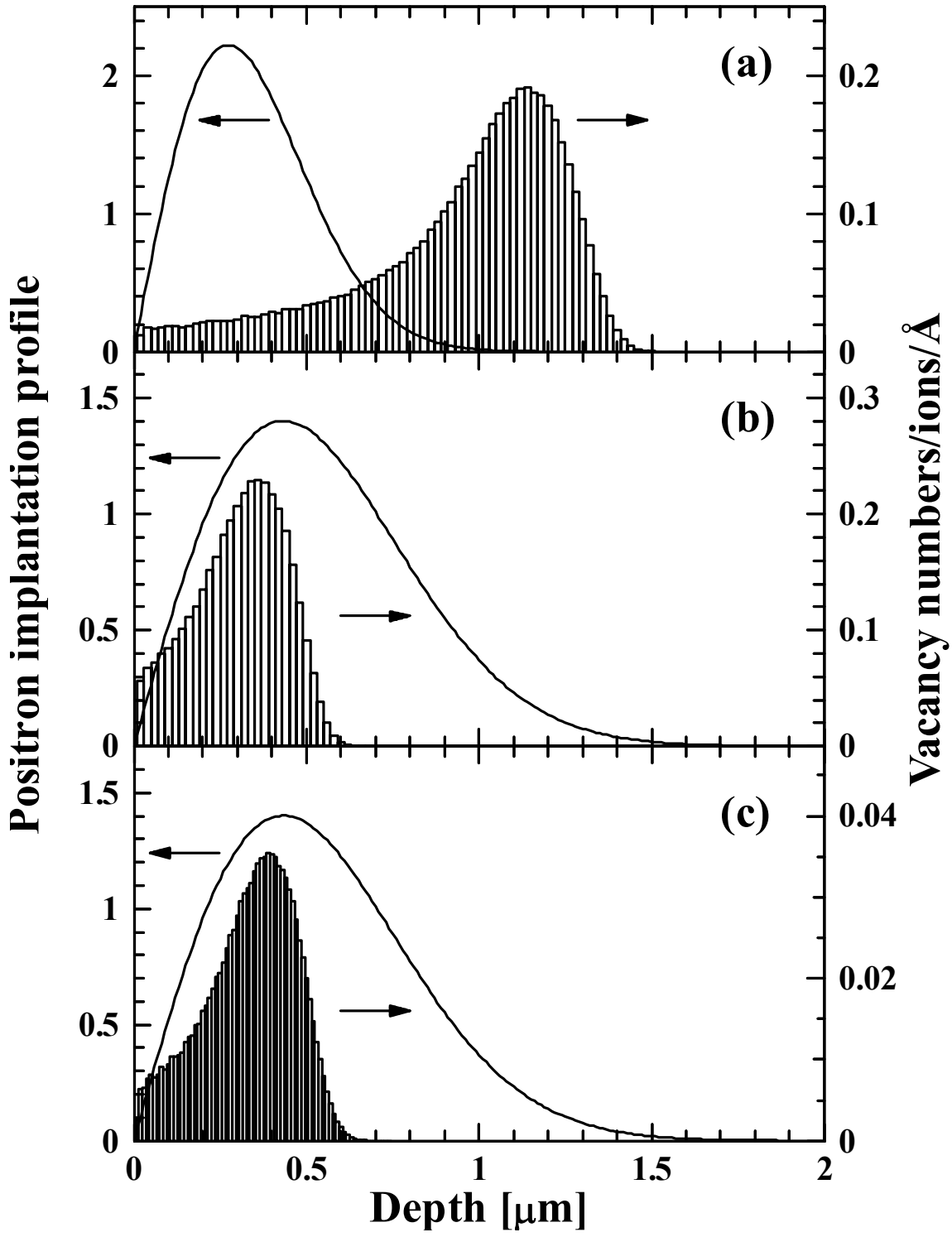

Figure 1 Tsuchida *et al*.

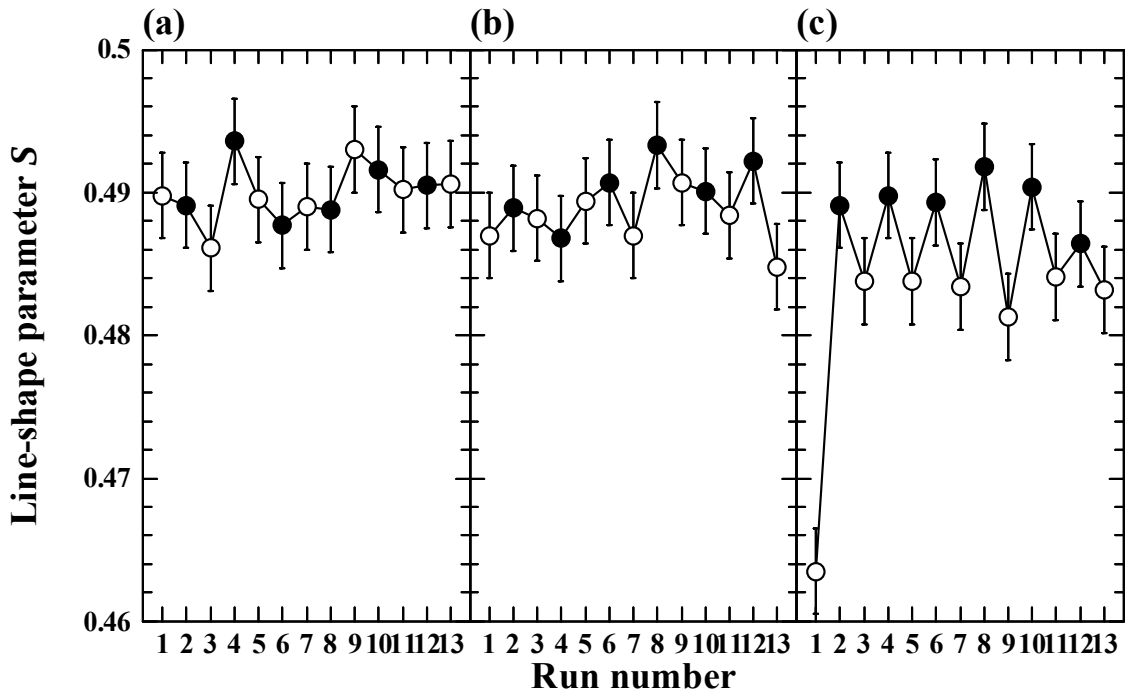

Figure 2 Tsuchida *et al*.

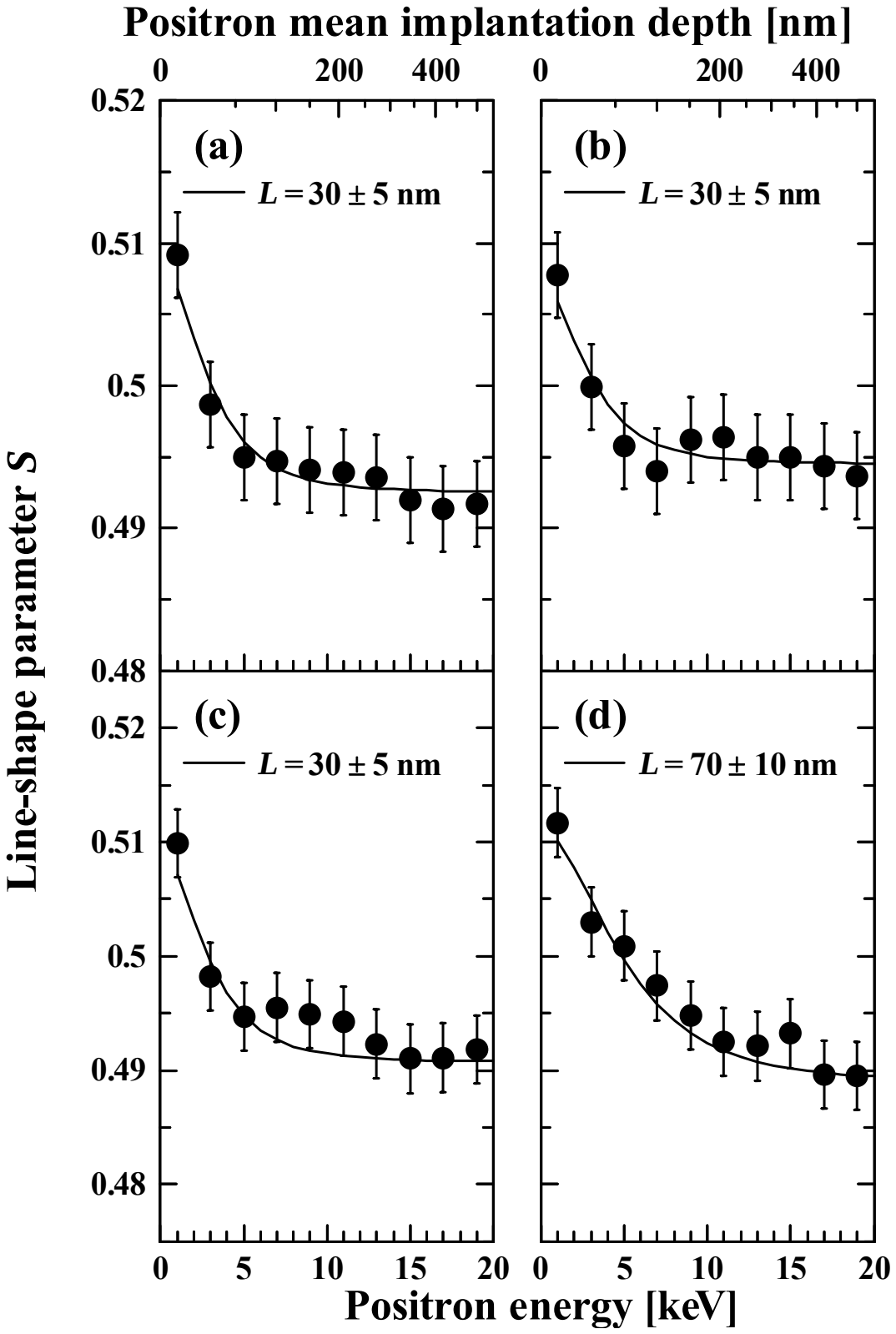

Figure 3 Tsuchida *et al.*